9110 *Inorg. Chem.* **2010**, *49*, 9110–9112
DOI: 10.1021/ic1015862

Inorganic Chemistry
Communication

Antimony Tin Oxide (ATO) Nanoparticle Formation from H_2O_2 Solutions: a New Generic Film Coating from Basic Solutions

Sergey Sladkevich,[†] Alexey A. Mikhaylov,[‡] Petr V. Prikhodchenko,*[,†,‡] Tatiana A. Tripol'skaya,[‡] and Ovadia Lev*[,†]

[†]*The Casali Institute of Applied Chemistry, The Institute of Chemistry, The Hebrew University of Jerusalem, Jerusalem 91904, Israel, and* [‡]*Kurnakov Institute of General and Inorganic Chemistry, Russian Academy of Sciences, Leninskii prosp. 31, Moscow 119991, Russia*

Received August 5, 2010

A generic method for conductive film coating of minerals and acid-sensitive materials by antimony-doped tin oxide (ATO) is introduced. The coating was performed from a hydrogen peroxide stabilized stannate and antimonate precursor solution. This is the first demonstration of ATO coating from an organic ligand-free solution. Uniform coating of different clays and other irregular configurations by monosized 5 nm ATO particles was demonstrated. The deposition mechanism and the observed preference for mineral surface coating over homogeneous agglomeration of the tin oxide particles are explained by a hydrogen peroxide capping mechanism and hydrogen bonding of the hydroperoxo nanoparticles to the H_2O_2-activated mineral surfaces.

Doped tin oxide coatings are receiving considerable scientific attention as future materials for sensors, catalysis, smart (heated) windows, and touch panel displays, voltage-dependent resistors, and LED devices, and they are also most promising for future solar cells and especially for polymer solar cells.[1] Diverse methods for particle and nanoparticle tin oxide formation and surface coatings have emerged.[2] Classification of the wet (doped as well as undoped) tin oxide coating methods reveals that they either are all produced in acidic media, usually from chloro or alkoxy precursors (followed by an annealing step),[3] or are made of preformed, stabilized nanocrystalline dispersions.[4] Although tin oxide nanoparticles and hollow spheres were prepared from hydroxostannate,[5] as far as we know, there is no report on the production of antimony-doped tin oxide (ATO) nanoparticles from a basic solution. ATO coatings from basic solutions are also still a challenge, and to date, there is no protocol for the production of ATO coatings from basic media, despite the importance of the coating of acid-sensitive materials by nanoparticulate ATO films.

We demonstrate a generic method for the coating of different surfaces, including acid-sensitive crystals ($LiNbO_3$ and calcite) from an organic, ligand-free, stable hydroperoxo-stannate and -antimonate solution. The method has an advantage for the coating of small entities because (nano)-particle formation takes place exclusively on surfaces, and we did not observe particle growth in the solution. The coating is comprised of <10 nm nanocrystalline material, which is favorable for catalysis and optical applications. We demonstrate the new protocol for the coating of Muscovite clays by ATO nanoparticles. Good conductivity of the composite-coated clay materials (ca. 15 Ω cm) was achieved. In the following, we shall describe briefly the coating protocol, demonstrate its compatibility with a wide range of substrates, and address in detail the coating of only one substrate, Muscovite. The coating mechanism is discussed in view of the recently acquired understanding of hydroperoxostannate chemistry.

The precursor solution was prepared by mixing aqueous tetramethylammonium hexahydroxostannate and hexahydroxoantimonate solutions. After the addition of 15% hydrogen peroxide, the solution remained translucent. ATO coating was done by immersion of the substrates into the H_2O_2 precursor solution and the addition of excess ethanol.

*To whom correspondence should be addressed. E-mail: ovadia@vms.huji.ac.il (O.L.), Prikhman@gmail.com (P.V.P.).

(1) (a) Steim, R.; Kogler, F. R.; Brabec, C. J. *J. Mater. Chem.* **2010**, *20*, 2499. (b) Helgesen, M.; Sondergaard, R.; Krebs, F. C. *J. Mater. Chem.* **2010**, *20*, 36. (c) Granqvist, C. G. *Sol. Energy Mater. Sol. Cells* **2007**, *91*, 1529. (d) Chiu, H. C.; Yeh, C. S. *J. Phys. Chem. C* **2007**, *111*, 7256. (e) Choi, M. C.; Kim, Y.; Ha, C. S. *Prog. Polym. Sci.* **2008**, *33*, 581. (f) Su, Y. Y.; Chen, H.; Wang, Z. M.; Lv, Y. *Appl. Spectrosc. Rev.* **2007**, *42*, 139. (g) Bueno, P. R.; Varela, J. A.; Longo, E. *J. Eur. Ceram. Soc.* **2008**, *28*, 505. (h) Batzill, M.; Diebold, U. *Prog. Surf. Sci.* **2005**, *79*, 47. (i) Krebs, F. C.; Tromholt, T.; Jorgensen, M. *Nanoscale* **2010**, *2*, 873.

(2) (a) Choy, K. L. *Prog. Mater. Sci.* **2003**, *48*, 57. (b) Granqvist, C. G.; Hultaker, A. *Thin Solid Films* **2002**, *411*, 1. (c) Xi, G.; Ye, J. *Inorg. Chem.* **2010**, *49*, 2302. (d) Wang, Y.-F.; Lei, B.-X.; Hou, Y.-F.; Zhao, W.-X.; Liang, C.-L.; Su, C.-Y.; Kuang, D.-B. *Inorg. Chem.* **2010**, *49*, 1679.

(3) (a) Santilli, C. V.; Rizzato, A. P.; Pulcinelli, S. H.; Craievich, A. F. *Phys. Rev. B* **2007**, *75*, 205335. (b) Hu, P. W.; Yang, H. M. *Appl. Clay Sci.* **2010**, *48*, 368. (c) Nütz, T.; Haase, M. *J. Phys. Chem. B* **2000**, *104*, 8430.

(4) Muller, V.; Rasp, M.; Rathousky, J.; Schutz, B.; Niederberger, M.; Fattakhova-Rohlfing, D. *Small* **2010**, *6*, 633.

(5) (a) Juttukonda, V.; Paddock, R. L.; Raymond, J. E.; Denomme, D.; Richardson., A. E.; Slusher, L. E.; Fahlman, B. D. *J. Am. Chem. Soc.* **2006**, *128*, 420. (b) Urade, V. N.; Hillhouse, H. W. *J. Phys. Chem. B* **2005**, *109*, 10538. (c) Lou, X. W.; Wang, Y.; Yuan, C. L.; Lee, J. Y.; Archer, L. A. *Adv. Mater.* **2006**, *18*, 2325.

Published on Web 09/23/2010

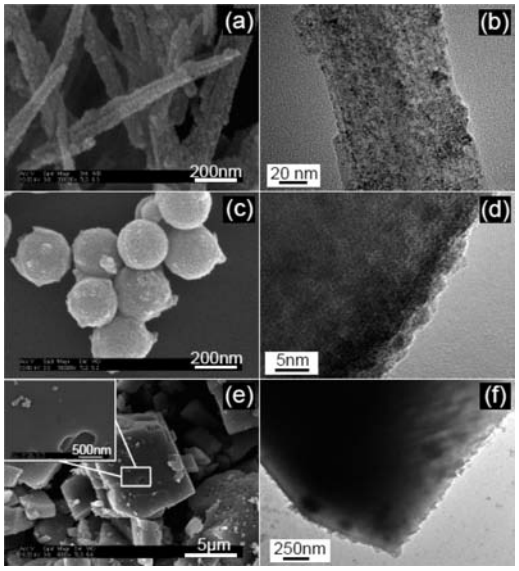

Figure 1. SEM (left) and TEM (right) micrographs of ATO-coated sepiolite (a and b), sol−gel silica powder (c and d), and calcite (e and f). See Figure S1 in the Supporting Information for $LiNbO_3$ and kaolin coatings.

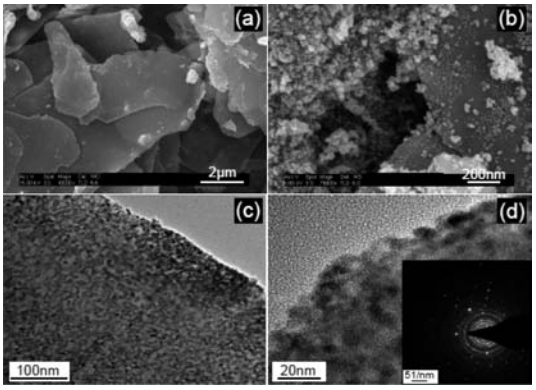

Figure 2. SEM micrographs of ATO-coated mica by the hydroperoxostannate and -antimonate route (a) and from hydrogen peroxide free precursors (b). Frames c and d show the TEM micrographs of ATO-coated mica, and the electron diffraction pattern is given in the inset.

The coated material was filtered or centrifuged out, washed with ethanol, and calcined. The room temperature coated material contained several percents of active oxygen and some organic residue, but these were lost in the heat treatment. Following the same procedure but without adding peroxide resulted in ATO agglomerate formation rather than thin film coating.

Generality. To demonstrate that the coating procedure is indeed general, we have coated six different crystalline and amorphous materials. The transmission electron microscopy (TEM) and scanning electron microscopy (SEM) micrographs of coated and heat-treated sepiolite, a magnesium silicate, one-dimensional clay are depicted in Figure 1a,b, the relevant pictures for Muscovite, a potassium mica, are depicted in Figure 2, and the micrographs of kaolin, a two-dimensional aluminosilicate, and $LiNbO_3$ are depicted in Figure S1 in the Supporting Information. The SEM pictures (first column) show a uniform coating of all three clays. The figures also show that the ATO is exclusively attached to the clays, and it is not agglomerated elsewhere. The relevant TEM micrographs (parts b, d, and f of Figure 1, parts c and d

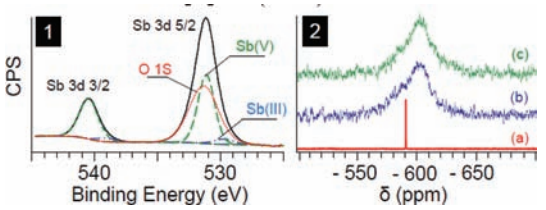

Figure 3. (1) XPS signal of antimony in 800 °C treated ATO-coated mica with the deconvoluted O 1s antimony (III) and antimony (V) signals. (2) ^{119}Sn NMR spectra of (a) hydroxostannate aqueous solution, (b) peroxystannate solution, and (c) peroxystannate and antimonate solutions in 15% H_2O_2.

of Figure 2, and Figure S1 in the Supporting Information), taken at the edges of the different materials, show approximately 5 nm crystalline particles almost uniform in size, regardless of the substrate used. For generality, we have also included sol−gel-derived nanoparticles that were prepared by a sol−gel microemulsion process. The ATO-coated silica gel particles are also uniformly coated, and again the 5 nm crystalline coating can be readily observed in the periphery of the 200 nm spheres. We have also coated two acid-sensitive powders: lithium niobate, which is widely used in optoelectronics and for nonlinear optics, and calcite, a birefringent material of electrooptical importance. Again, and despite the lack of external silica tetrahedra or surface silanols in these minerals, the coating took place exclusively on the minerals, and the size of the crystallite was again around 5 nm. Figure S1 in the Supporting Information shows the local diffraction pattern of the ATO-coated $LiNbO_3$. The single-crystal diffraction dots of $LiNbO_3$ and the multicrystalline diffraction rings of the ATO nanocrystals are apparent. After being convinced that the procedure is generic and even the acid-sensitive optical materials can be coated by the ATO particles, we prefer to refrain from further discussion of all six samples and discuss in more detail the coating of only one substrate, Muscovite clays.

ATO-Coated Mica. Preparation details are described in the Supporting Information. SEM micrographs of the bare (Figure S1 in the Supporting Information) and ATO-coated mica (Figures 2a and S1 in the Supporting Information) are presented. Uniform coating of all other minerals by ca 5 nm nanocrystalline ATO is demonstrated in the TEM micrographs (Figure 2c,d). In comparison, our attempts to produce ATO coatings from the hydroxostannate and -antimonate precursors did not result in any precipitation after alcohol treatment. Mild acidification yielded only an agglomerated material that did not coat the mica surface (Figure 2b).

X-ray photoelectron spectroscopy (XPS) studies of the 800 °C treated ATO-coated mica reveal the Sn $3d_{3/2}$ binding energy levels of tin (IV) at 495.73 eV and Sn $3d_{5/2}$ at 487.32 eV. The Sb $3d_{3/2}$ peak (Figure 3, left side) can be deconvoluted to two peaks at 539.06 and 540.46 eV corresponding to antimony (III) and antimony (V) oxides, respectively.[6] Deconvolution of the $3d_{5/2}$ peak reveals two peaks at 529.72 and 531.12 eV matching the $3d_{3/2}$ signals, in addition to an overlapping broad O 1s signal. The ratio between the Sb $3d_{3/2}$ and Sb $3d_{5/2}$ signals was, as expected, 2:3. The molar Sb/Sn ratio by XPS studies was 12:88. The ratio between antimony (V) and antimony (III) by XPS studies was 11:1. X-ray diffraction

(6) Izquierdo, R.; Sacher, E.; Yelon, A. *Appl. Surf. Sci.* **1989**, *40*, 175.

(XRD) studies of 800 °C calcined and room temperature prepared ATO-coated mica are depicted in Figure S2 in the Supporting Information. The room temperature coated mica shows some shallow, broad peaks at $\theta = 50-55°$ and 25−35° corresponding to amorphous tin oxide. Heat treatment resulted in the formation of a crystalline SnO_2 phase.

Mechanistic Aspects. Because tin oxide is the dominant species in ATO, it is worthwhile to start this discussion with its chemistry. The starting tetramethylammonium hexahydroxostannate solution is at high pH, and the dominant tin species under these conditions is the monomer anions. The ^{119}Sn NMR spectrum [Figure 3 (2,a)] indeed shows only a single sharp signal with chemical shift $\delta = -590.5$ ppm, corresponding to the hydroxostannate anion $[Sn(OH)_6]^{2-}$.[7] When hydrogen peroxide is added, it acts in two ways: (a) It reduces the pH. The addition of 20% hydrogen peroxide to a 1 M stannate solution decreases the pH (as measured by the pH electrode) from 12.6 to 8.4. (b) Hydroperoxo groups reversibly substitute hydroxo ligands. This is apparent by the formation of $[Sn(OOH)_6]^{2-}$ at high H_2O_2 concentrations. ^{119}Sn NMR studies have proven that ligand exchange takes place reversibly. The exchange is observable already at 1% hydrogen peroxide, and at ca. 90% H_2O_2, the most dominant dissolved species is $[Sn(OOH)_6]^{2-}$.[8] In addition, crystalline alkali-metal hydroperoxostannates were isolated from H_2O_2-rich (>70%) solutions.[9]

Lowering the pH of the hydroxystannate solution to near pH 9 would have resulted in the immediate precipitation of hydroxo-bridged stannate. However, the hydroperoxo−hydroxo ligand exchange counteracts the polymerization process. Peroxy-bridged (i.e., hydroperoxo or peroxo) stannate is not likely to form at this hydrogen peroxide concentration and pH range. Our own extensive investigation of peroxystannate nanoparticles (by ^{119}Sn NMR, XPS, FTIR, and Raman spectroscopies) failed to show any spectral hint for peroxo or hydroperoxo bridging.[8] The sum of the effects of $H_2O_2-H_2O$ ligand exchange and the pH decrease caused by the addition of hydrogen peroxide to the tin solution results in the formation of tin oligomers rather than precipitation [Scheme 1 and Figure 3(2.b)]. In a way, hydrogen peroxide acts as a capping agent that prevents full condensation. The broad ^{119}Sn NMR signal of Figure 3(2.b) proves oligomer formation. The NMR signal parameters of Figure 3(2.b) are close to the reported signal of hydroxo-bridged oligomers that were obtained by tin chloride hydrolysis in a peroxide-free solution,[10] which also supports hydroxo bridging.

The mechanism outlined thus far explains the formation of a stable translucent precursor solution, but it does not explain, as yet, the preferential coating of mica. We believe

Scheme 1. Tin Oxide Nanoparticle Formation, Hydrogen Peroxide Stabilization, and Preferential Deposition on Mineral Surfaces

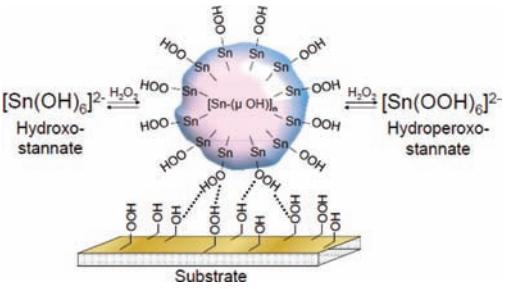

that the preferential attachment of the oligomers to the silica tetrahedra is by the formation of hydrogen bonds between the terminal ("capping") hydroperoxo groups on the tin oligomers and the silanol groups. It is also possible that hydroperoxo−hydroxo ligand exchange further activates the surface. Hydroperoxide silicate adduct formation was reported by Żegliński et al.,[11] and H_2O_2−clay ligation was demonstrated by us.[12] The proposed mechanism explains equally well the preferential coating of the other clay minerals (kaolin and sepiolite) and of silica gel, and, of course, calcium carbonate has a high propensity for hydrogen bonding with hydroperoxo groups (as is apparent in the structure of sodium percarbonate).[13]

The role of the antimonate has not been discussed thus far. Hydroxyantimonate has also octahedral coordination,[14] and several articles have demonstrated interaction between antimonates and hydrogen peroxide.[15] Therefore, we assume here that the interaction of antimonate with hydrogen peroxide is similar to that of stannate. Indeed, the NMR spectra of Figure 3(2.c) in the presence of antimony and in its absence [Figure 3(2.b)] are very similar, suggesting that the tin environment is not altered considerably by the addition of antimony oxide. The differences between the two elements may substantially affect the degree of mixing of the tin and antimony oxides, but this is a subject of a different account.

Acknowledgment. We thank the Israel Ministry of Science and the Russian Foundation for Basic Research (Grants 08-03-00537, 09-03-92476, and 09-03-12151). We thank Drs. D. Krut'ko and M. Fedotov for useful discussions. Nanocharacterization was conducted in the Harwey M. Kreuger Center for Nanoscience and Nanotechnology of the Hebrew University.

Supporting Information Available: Experimental details, SEM and TEM of $LiNbO_3$, kaolin, and mica, and XRD studies of coated mica. This material is available free of charge via the Internet at http://pubs.acs.org.

(7) Burke, J. J.; Lauterbur, P. C. *J. Am. Chem. Soc.* **1961**, *83*, 326.
(8) Sladkevich, S.; Gutkin, V.; Lev, O.; Legurova, E. A.; Khabibulin, D. F.; Fedotov, M. A.; Uvarov, V.; Tripol'skaya, T. A.; Prikhodchenko, P. V. *J. Sol−Gel Sci. Technol.* **2009**, *50*, 229.
(9) (a) Churakov, A. V.; Sladkevich, S.; Lev, O.; Tripol'skaya, T. A.; Prikhodchenko, P. V. *Inorg. Chem.* **2010**, *49*, 4762. (b) Prikhodchenko, P. V.; Churakov, A. V.; Novgorodov, B. N.; Kochubei, D. I.; Muravlev, Yu. B.; Ippolitov, E. G. *Russ. J. Inorg. Chem.* **2003**, *48*, 16. (c) Churakov, A. V.; Prikhodchenko, P. V.; Ippolitov, E. G.; Antipin, M. Yu.; Russ. J. *Inorg. Chem.* **2002**, *47*, 68–71. (d) Ippolitov, E. G. Tripol'skaya, T. A.; Prikhodchenko, P. V.; Pankratov, D. A.; Russ. J. *Inorg. Chem.* **2001**, *46*, 851–857.
(10) Taylor, M. J.; Coddington, J. M. *Polyhedron* **1992**, *11*, 1531.
(11) Żegliński, J.; Cabaj, A.; Strankowski, M.; Czerniak, J.; Haponiuk, J. T. *Colloids Surf., B* **2007**, *54*, 165.
(12) Tripol'skaya, T. A.; Pilipenko, G. P.; Legurova, E. A.; Pokhabova, I. V.; Prikhodchenko, P. V. *Russ. J. Inorg. Chem.* **2009**, *54*, 512.
(13) Pritchard, R. G.; Islam, E. *Acta Crystallogr., Sect. B: Struct. Sci.* **2003**, *59*, 596.
(14) (a) Asai, T. *Bull. Chem. Soc. Jpn.* **1975**, *48*, 2677. (b) Friedrich, A.; Wildner, M.; Tillmanns, E.; Merz, P. L. *Am. Mineral.* **2000**, *85*, 593.
(15) (a) Siebert, H. *Z. Anorg. Allg. Chem.* **1959**, *301*, 316. (b) Ippolitov, E. G.; Tripol'skaya, T. A.; Pilipenko, G. P. *Zh. Neorg. Khim.* **1998**, *43*, 370. (c) Brazdil, J. F.; Toft, M. A.; Bartek, J. P.; Teller, R. G.; Cyngier, R. M. *Chem. Mater.* **1998**, *10*, 4100.